# 3D TRACK-KEEPING CONTROL FOR AUTONOMOUS UNDERWATER VEHICLE

**Bian Xin-Qian**
**Best Sea Assembly Institute**
Harbin Engineering University, China
bianxq@public.hr.hl.cn

**Wang Wei**
**Best Sea Assembly Institute**
Harbin Engineering University, China
weiwangaddress@mail.china.com

**Abstract**

In this paper, 3D track-keeping control method for Autonomous Underwater Vehicle (AUV) with and without the influence of ocean current is investigated. The design of an autopilot for the control of underwater vehicles is of interest both from the view of motion stabilization as well as maneuverability and path tracking performance. Because the system to be controlled is highly nonlinear, coupled, and there is a good deal of parameter uncertainty and variation with operational conditions, an approach is used to divide the control system into three subsystems. The first is to control the speed of AUV. The second is to control the heading and the tracking error on the horizontal plane. And the third is to control the pitch and the tracking error on the vertical plane. The results of computer simulation show that the autopilot works properly, it can capture the current waypoint and turn to track the next path automatically.

## Introduction

To widen the range of application of Autonomous Underwater Vehicle both in industrial application and in environmental survey, AUV need to have higher intelligence. It is important to construct a reliable representation of underwater environment to plan viable trajectories leading to safe mission execution. AUV will track the planning paths precisely. In this paper, an autopilot based on the control of heading and pitch is designed. To compensate the influence of modeling nonlinearity, uncertainty and disturbances, two sliding mode controllers would be designed to control heading and pitch angle separately. To achieve track-keeping precisely, the guidance controllers are also designed to adjust the heading and pitch angle. Thus the control system can control the heading and pitch of AUV dependently, and it also can realize the 3D track-keeping with and without the current.

## 1. Mathematical model in Six degree of freedom

According to the shape and the experimental data of wind tunnel, we take the origin of the vehicle-fixed coordinate in the centroid and proceed appropriate simplification. The six dimensional equations of motion for hydrodynamically shaped underwater vehicles can be represented as

$$\begin{aligned} m[\dot{u} - vr + wq] &= 0.5\rho L^3[X'_{\dot{u}}\dot{u} + X'_{wq}wq + X'_{vr}vr] \\ &+ 0.5\rho L^2[X'_{uu}uu + X'_{vv}v^2 + X'_{ww}w^2] + 0.5\rho L^4[X'_{rr}r^2 \\ &+ X'_{qq}q^2 + X'_{pr}pr] - (W - B)\sin\theta \\ &+ 0.5\rho L^2[X'_{\delta r\delta r}\delta_r^2 + X'_{\delta s\delta s}\delta_s^2] + T_{prop} \end{aligned} \quad (1)$$

$$\begin{aligned} m[\dot{v} + ur - wp] &= 0.5\rho L^4[Y'_{\dot{r}}\dot{r} + Y'_{pq}pq + Y'_{qr}qr \\ &+ Y'_{r|r|}r\,|r\,|] + 0.5\rho L^3[Y'_{\dot{v}}\dot{v} + Y'_{ur}ur + Y'_{wp}wp + Y'_{vq}vq \\ &+ Y'_{v|r|}v\,|r\,|] + 0.5\rho L^2[Y'_{uv}uv + Y'_{vw}vw + Y'_{v|v|}v\,|v\,|] \\ &+ (W - B)\cos\theta\,\sin\varphi + 0.5\rho L^2 Y'_{\delta r}u^2\delta r \end{aligned} \quad (2)$$

$$
\begin{aligned}
& m[\dot{w} - uq + vp] = 0.5 r L^4 [Z'_{\dot{q}} \dot{q} + Z'_{rp} rp + Z'_{pp} p^2 \\
& + Z'_{q|q|} q|q|] + 0.5 r L^3 [Z'_{\dot{w}} \dot{w} + Z'_{vp} vp + Z'_{uq} uq \\
& + Z'_{w|q|} w|q|] + 0.5 r L^2 [Z'_{uw} uw + Z'_{w|w|} w|w|] \\
& + (W - B)\cos q \cos j + 0.5 r L^2 Z'_{ds} u^2 d s
\end{aligned} \tag{3}
$$

$$
\begin{aligned}
& I_x \dot{p} + (I_z - I_y) qr = 0.5 r L^5 [K'_{\dot{p}} \dot{p} + K'_{pq} pq \\
& + K'_{qr} qr + K'_{p|p|} p|p|] + 0.5 r L^4 [K'_{\dot{v}} \dot{v} + K'_{wp} wp \\
& + K'_{wr} wr + K'_{up} up + K'_{vq} vq] + 0.5 r L^3 [K'_{v} uv \\
& + K'_{v|v|} v|v| + K'_{vw} vw] + Z_B B \cos q \sin j \\
& + 0.5 r L^3 u^2 K'_{dr} d r
\end{aligned} \tag{4}
$$

$$
\begin{aligned}
& I_y \dot{q} + (I_x - I_z) pr = 0.5 r L^5 [M'_{\dot{q}} \dot{q} + M'_{pp} p^2 \\
& + M'_{rr} r^2 + M'_{pr} pr + M'_{q|q|} q|q|] + 0.5 r L^4 [M'_{\dot{w}} \dot{w} \\
& + M'_{uq} uq + M'_{vr} vr + M'_{|w|q} |w| q + M'_{vp} vp] \\
& + 0.5 r L^3 [M'_{uw} uw + M'_{w|w|} w|w|] + Z_B B \sin q \\
& + 0.5 r L^2 M'_{ds} u^2 d s
\end{aligned} \tag{5}
$$

$$
\begin{aligned}
& I_z \dot{r} + (I_y - I_X) pq = 0.5 r L^5 [N'_{\dot{r}} \dot{r} + N'_{pq} pq \\
& + N'_{r|r|} r|r| + N'_{qr} qr] + 0.5 r L^4 [N'_{\dot{v}} \dot{v} + N'_{vq} vq \\
& + N'_{wp} wp + N'_{ur} ur + N'_{|v|r} |v| r + N'_{v|r|} v|r|] \\
& + 0.5 r L^3 [N'_{v} u v + N'_{v|v|} v|v| + N'_{vw} vw] \\
& + 0.5 r L^3 N'_{dr} u^2 d r
\end{aligned} \tag{6}
$$

the nomenclature is the same as those in reference [1].

## 2. The principle of track-keeping control system

Figure 1 shows the principle of 3D track-keeping. At the beginning, according to the nautical chart, AUV will plan paths. Then the computer will calculate $y_0$ (the course of the path) and $q_0$ (the angle between the path and the horizontal plane). As shown in Fig. 2, the distance $d1$ is the track error on the horizontal plane, it is used as the input of heading guidance controller. $y'$ is the output of heading guidance controller. As shown in Fig. 3, the distance $d2$ is the track error on the vertical plane. It is used as the input of pitch guidance controller. $q'$ is the output of this guidance controller. $y_{com} = y_0 - y'$ is the command value of the heading controller and $q_{com} = q_0 - q'$ is the command value of the pitch controller. The system to be controlled has been divided into two subsystems. Two sliding mode control laws are designed to control heading and pitch.

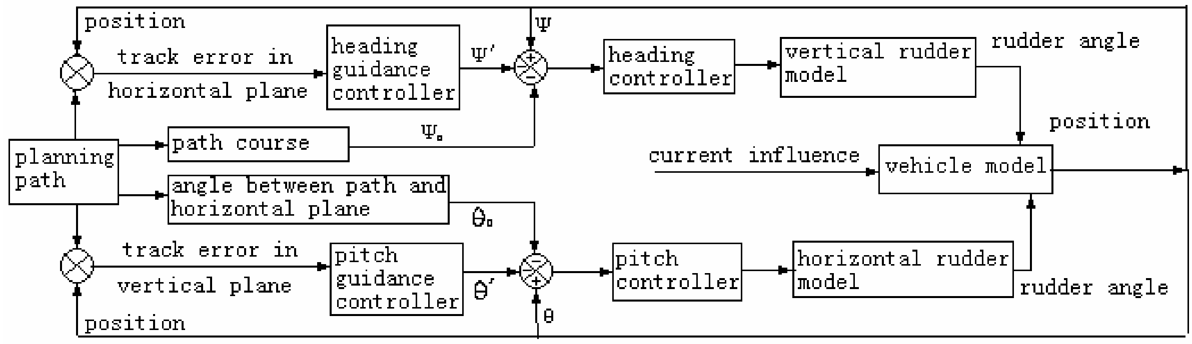


Fig.1 Principle of 3D track-keeping.

### 2.1 Sliding mode heading controller

Eq.(2), Eq.(6) and equation of Euler angle rate $\dot{r}$ are linearized at the speed $u_0$, which the linear terms are collected and residuals act as unknown forcing terms

$$
\begin{bmatrix} 1 & 0 & 0 \\ 0 & m_{22} & m_{23} \\ 0 & m_{32} & m_{33} \end{bmatrix}
\begin{bmatrix} \dot{y}(t) \\ \dot{v}(t) \\ \dot{r}(t) \end{bmatrix}
=
\begin{bmatrix} 0 & 0 & 1 \\ 0 & A_{22} & A_{23} \\ 0 & A_{32} & A_{33} \end{bmatrix}
\begin{bmatrix} y(t) \\ v(t) \\ r(t) \end{bmatrix}
+
\begin{bmatrix} 0 \\ B_2 \\ B_3 \end{bmatrix} d_r(t)
+
\begin{bmatrix} D_1(t) \\ D_2(t) \\ D_3(t) \end{bmatrix} \tag{7}
$$

where $m_{22} = m - 0.5 r L^3 Y'_{\dot{v}}$, $m_{23} = -0.5 r L^4 Y'_{\dot{r}}$,

$m_{32} = -0.5 r L^4 N'_{\dot{v}}$, $m_{33} = I_z - 0.5 r L^5 N'_{\dot{r}}$,

$A_{22} = 0.5 r L^2 u_0 Y'_v$, $A_{23} = -m u_0 r + 0.5 r L^3 u_0 Y'_r$,

$A_{32} = 0.5 r L^3 u_0 N'_v$, $A_{33} = 0.5 r L^4 u_0 N'_r$,

$B_2 = 0.5 r L^2 u_0^2 Y'_{dr}$, $B_3 = 0.5 r L^3 u_0^2 N'_{dr}$. $D_1(t)$, $D_2(t)$ and $D_3(t)$ contain the differences between linear and nonlinear accelerations and velocities, uncertain and disturbance. $D_1(t)$ , $D_2(t)$ and $D_3(t)$ are uncertain in general but restricted for bounded motion inputs.

Defining the sliding surface for heading control as

$$s_1(\mathbf{x}) = \mathbf{s}\mathbf{x} \tag{8}$$

To achieve good dynamic characteristics, the value to place the sliding poles of the heading system at the desired extremity gathers. The sliding surface is then formed as a linear combination of state variable errors in the usual way. Ignoring any nonzero yaw rate command $r_{com}$ and speed command $v_{com}$ , the sliding surface polynomial using a commanded heading angle $y_{com}$

$$s_1(\mathbf{x}) = 0.5847(y - y_{com}) + 0.0297v + r \tag{9}$$

and the corresponding control law for the vertical rudder is

$$d_r = -0.312v - 0.781r + 4.22k\,\mathrm{sign}(s_1) \tag{10}$$

where $k$=0.48, nonlinear control gain of controller.

**2.2 Heading guidance controller**

As shown in Fig. 2, along the planning path AB, the horizontal plane is divided into two parts. The value of track error $d1$ is positive when AUV locates the right side of line AB and the value of $d1$ is negative when AUV locates the left side of line AB. When the absolute value of $d1$ is larger than $D_{max}$ , a proportional controller will be adopted to lead the AUV quickly close to the planning path AB. When AUV is close enough to the path, a PID controller will be adopted. This multi-mode control method is of some advantage. The PID controller can eliminate steady state error arose by the ocean current.

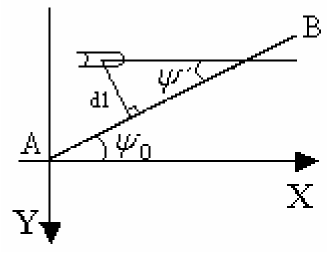


Fig.2 **Heading guidance**

$$y' = K_{p1}d, \qquad |d| > D_{max} \tag{11}$$

$$y' = K_{P1}d + K_{D1}\dot{d} + K_{I1}\int d \bullet dt, \quad |d| \geq D_{max} \tag{12}$$

where $d$ is the track error $d1$, $D_{max}$ =5m, the range of $y'$ is limited to $\pm 45^\circ$ , and $y_0$ is the course of planning path.

**2.3 Sliding mode pitch controller**

As the heading controller, the state space is made of Eq.(3), Eq.(5) and equation of Euler angle rate $\dot{q}$ . To eliminate the steady state error, an integral control term $\dot{q}_I = q$ is adding to the state space representation.

$$\begin{bmatrix} 1 & 0 & 0 & 0 \\ 0 & 1 & 0 & 0 \\ 0 & 0 & m_{33} & m_{34} \\ 0 & 0 & m_{43} & m_{44} \end{bmatrix} \begin{bmatrix} \dot{q}_I \\ \dot{q} \\ \dot{w} \\ \dot{q} \end{bmatrix} = \begin{bmatrix} 0 & 1 & 0 & 0 \\ 0 & 0 & 0 & 1 \\ 0 & A_{32} & A_{33} & A_{34} \\ 0 & 0 & A_{43} & A_{44} \end{bmatrix} \begin{bmatrix} q_I \\ q \\ w \\ q \end{bmatrix}$$

$$+ \begin{bmatrix} 0 \\ 0 \\ B_3 \\ B_4 \end{bmatrix} d_s + \begin{bmatrix} 0 \\ D_2(t) \\ D_3(t) \\ D_4(t) \end{bmatrix} \tag{13}$$

where $m_{33} = -0.5\,r L^4 M'_{\dot{w}}$, $m_{34} = I_y - 0.5\,r L^5 M'_{\dot{q}}$,

$m_{43} = m - 0.5\,r L^3 Z'_{\dot{w}}$ , $m_{44} = -0.5\,r L^4 Z'_{\dot{q}}$,

$A_{32} = Z_B W$ , $A_{33} = 0.5\,r L^4 Z'_q$,

$A_{34} = 0.5\,r L^4 u_0 M'_q$ , $A_{43} = 0.5\,r L^2 u_0 Z'_w$ . $D_1(t)$ , $D_2(t)$ and $D_3(t)$ contain the differences between linear and nonlinear accelerations and velocities, uncertain and disturbance. $D_1(t)$ , $D_2(t)$ and $D_3(t)$ are uncertain in general but restricted for bounded motion inputs.

Defining the sliding surface for pitch control as $s_2(\mathbf{x})$, the values to place the sliding poles of the system at desired extremity gathers become

$$s_2(\mathbf{x}) = 0.0898q_I + 0.557(q - q_{com}) - 0.0145w + q$$

(14)

and the pitch control law results in

$$d_s = 1.09(q - q_{com}) + 1.51w - 32.37q + 46.4k\,\mathrm{sign}(s_2) \quad (15)$$

where $k$=0.15, nonlinear control gain of controller.

### 2.4 pitch guidance controller

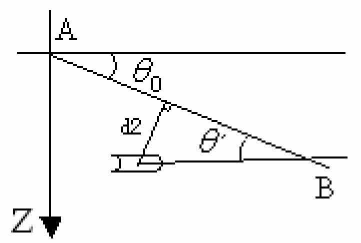


Fig.3 Pitch guidance

In Fig.3, the whole vertical plane is divided into two parts by the line AB. track error $d2$ on the vertical plane is positive when AUV is on the top area and d is negative when AUV is on the bottom. When the absolute value of $d2$ is larger than $D_{max}$, a proportional controller will be adopted to lead the AUV quickly close to the planning path AB. When AUV is close enough to the path, a PID controller must be adopted.

$$q' = K_{p2}d\ ,\ |d| > D_{\max} \quad (16)$$

$$q' = K_{P2}d + K_{D2}\dot{d} + K_{I2}\int d \cdot dt\ ,\ |d| \le D_{\max} \quad (17)$$

### 3. Computer Simulation results

The time step of simulation is 0.01s and the sample period of system is 0.5s.

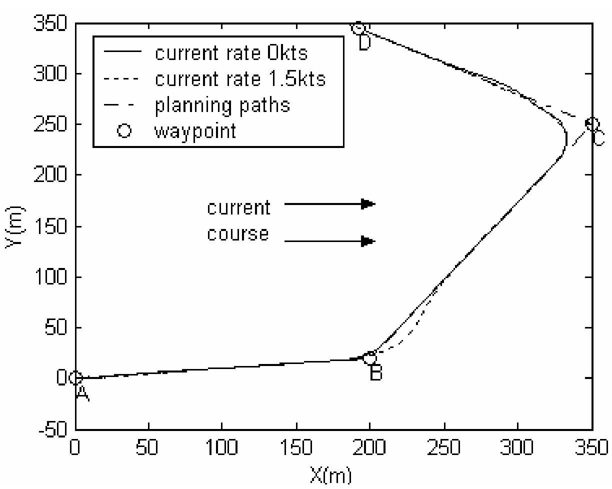


Fig.4 Track on the horizontal plane

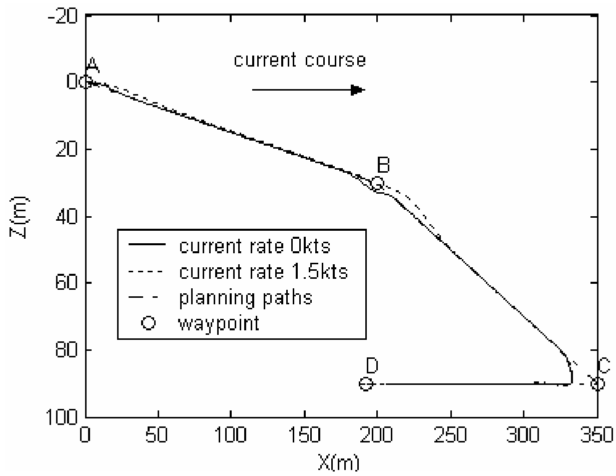


Fig.5 Track on the vertical plane

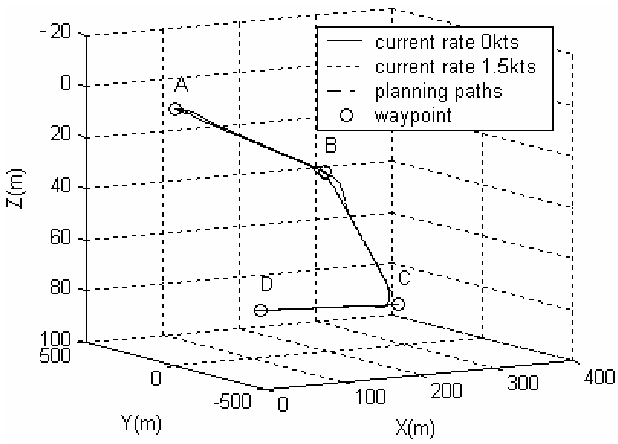


Fig.6 Track on the 3D space

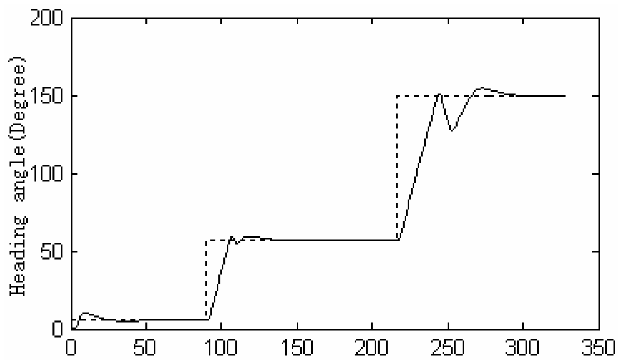


Fig.7 Heading response without current

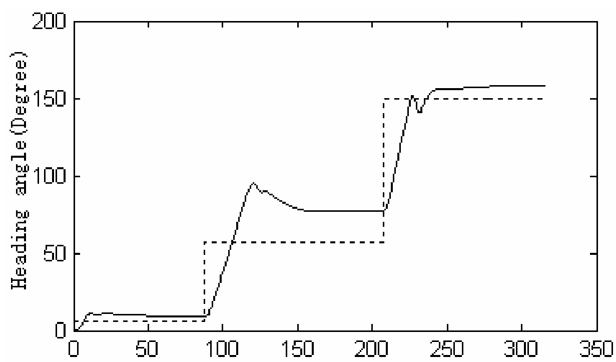

Fig.8 Heading response with current

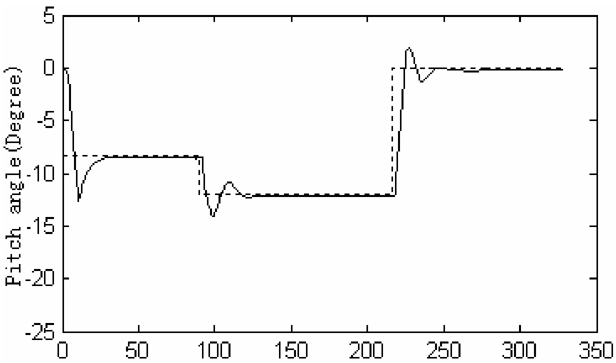


Fig.9 Pitch response without current

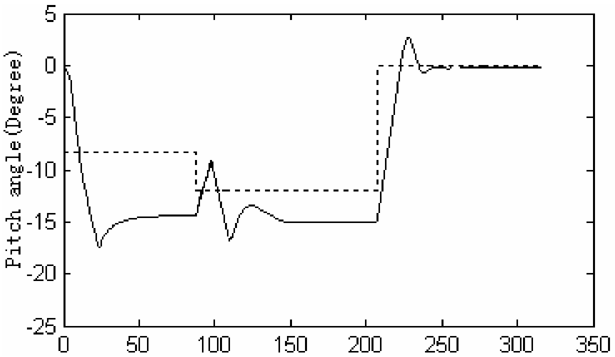


Fig.10 Pitch response with current

The paths in Figs.4, 5 and 6 are comprised of waypoints A, B, C and D. The solid line is the track line without the influence of ocean current, and the dashed line is the track line with the ocean current at 1.5 kn. From these three figures, it can be seen that the effect of track-keeping is good. AUV realizes track-keeping precisely.

Figure 7 and 8 show a comparison of heading angle response with and without the influence of ocean current. The dashed lines are the course of the planning path. The solid lines are real heading response. The figure 8 shows the influence of ocean current at 1.5kn. The vehicle tends to track the planning path. To compensate for the current, AUV will adjust a certain heading angle $y'$. The value of the adjusting heading angle will change with current rate and the angle between the course of planning path and the current. From Fig.4, we know the angle between the line BC and the current is larger than others. The influence of current is the largest for AUV on the path BC. So $y'$(the heading angle adjusted on the second path BC) is larger than others.

Figure 9 and 10 are the comparison of pitch angle response with and without current. The adjusting pith angle $q'$ is of the largest value on the first path. And $q'$ on the third path CD is near to zero because the third part of paths is depth keeping. That's to say, the influence to the pitch control of AUV is very small on third part.

## 4. Conclusion

In this paper, sliding mode method for heading and pitch control has been proposed. The method is generally suitable for a wide variety of nonlinear control problems although for flight conditions. A linear model for the sliding surface coefficient is used to make the design of controller easy. In particular, remarkable performance enhancements were attained by using multi-mode P and PID guidance algorithms. The algorithms were applied to adjust the heading and pitch angle. The simulation results show that this autopilot system works properly. It can capture the current waypoint and turn to track the next path automatically and realizes track-keeping precisely.

## References


[1] Hou-Tai Chen. Manipulation of the submarine[M]. National Defence Industry Press.

[2] HEALEY, A. J. and LIENARD, D. Multivariable sliding mode control for autonomous diving and steering of unmanned underwater vehicles[J]. IEEE Journal of Oceanic Engineering, 1993, 18( 3): 327-339.

[3] V.I. Utkin. Variable structure systems with sliding modes[J]. IEEE Trans. Automat. Contr., 1977, vol.22:, 212-222,

[4] Witt N A. Recent technological advance in the control and guidance of ships [J]. J Navigation, 1994, 47(2): 236-258.